Synthesis and evaluation of lipoic acid – donepezil hybrids for Alzheimer's disease using a straightforward strategy.

Vincent Luzet, Florentin Allemand, Chloé Richet, BarbaraDehecq, Alexandre Bonnet, Dominique Harakat, Lhassane Ismaïli, Bernard Refouvelet, Hélène Martin, Bruno Cardey, Marc Pudlo

Graphical Abstract

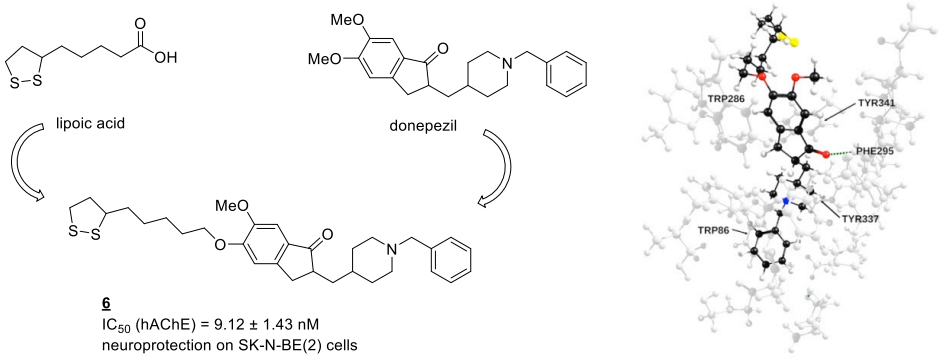

Abstract

Alzheimer disease is the most common form of dementia affecting elderly people. The decline in cognitive function is associated with a progressive loss of neurons and synaptic connections, especially in the cholinergic system and donepezil acetylcholinesterase inhibitor is used to increase the level of neurotransmitter.

Oxidative stress contributes to neurons damages and to the development of amyloid plaques and neurofibrillary tangles. Therefore, antioxidants are widely studied to mitigate the progression of Alzheimer's disease, and among these, lipoic acid has demonstrated a neuroprotective effect. Lipoic acid has been introduced in multi-targeted design ligand approaches but lipoic *N*-benzylpiperidine hybrids failed at inhibit acetylcholinesterase.

Here, we present the synthesis, the molecular modeling, and the evaluation of lipoic acid – donepezil hybrids based on O-desmethyldonepezil. Compound **6** displays inhibition of acetylcholinesterase with an median inhibitory concentration of 7.6 nM, comparable to that of donepezil and a notable neuroprotective effect, slightly better to that of lipoic acid.

It suggests that 6-O-desmethyldonepezil could serve a platform for the straightforward design of donepezil hybrids.

Introduction:

Alzheimer disease (AD) is the most common degenerative disorder affecting elderly people [1]. The disease is characterized by progressive memory loss and especially short-term memory. In later stages, AD leads to disturbances in speaking, ordering movement and visual recognition, resulting irremediably in loss of independence of the patient. Pathogenesis of AD remains unclear but it is widely accepted that senile plaques, consisting mainly of β-amyloid peptides and neurofibrillary tangles, linked to imbalance of kinase and phosphatase activities generate neuro-inflammation and neuronal dysfunctions [2]. Neuron depletion is especially massive in the cholinergic system and three of the four licensed drugs indicated in AD are acetylcholinesterase inhibitors (AChEI) namely donepezil, rivastigmine and galantamine that are most effective in the early stage. The fourth, memantine, is an antagonist of the N-methyl-D-aspartate receptor and is more effective in the later stage [3]. Current therapeutics only moderately delay the progression of symptoms [4] and there is a need for drugs that delay the progression of the disease.

Because of multifactorial physiopathology, the dominant paradigm guiding research for AD treatments is the multi-targeted design ligand (MTDL) considering that a drug with multiple actions will be more effective than a "one target" drug [5,6]. MTDL combined two or more pharmacophores with various properties including anti β-amyloid aggregation, β-secretase inhibition, monoamine oxidases inhibition, neuroprotective and antioxidant properties. Oxidative stress is a vector of damage and disease progression [7] and is mainly due to reactive oxygen species produced by mitochondrial dysregulation [8]. A wide amount of hybrids displaying antioxidant properties have been described [5]. Among these, lipoic acid (LA) was used very early in the MTDL approach [9–15] because of its efficacy for neutralizing ROS generated within mitochondria and disrupting the mechanism of downregulation involved in AD [16,17] including amyloidogenicity [18]. Moreover, clinical trials have demonstrated LA effectiveness and suggest a neuroprotective role against AD [19].

AChEI antioxidant hybrids are mostly based on tacrine [20] and the benzylpiperidine part of donepezil [21,22]. By this way, the indanone in donepezil is replaced by an aromatic ring with antioxidant activity, such as coumarin, ferulic acid, benzisoselenazolone, melatonin or hydroxyquinoline [23]. Lipoic *N*-benzylpiperidine hybrids target several objectives as β-

secretase-1, σ-1 receptor [13,24] and provide neuroprotective effect through antioxidant activity [9]. However, these compounds failed to display hAChE inhibition because of the lack of aromatic ring which is crucial for donepezil analogs binding to AChE peripheral anionic site [25]. Given this perspective, we investigated three derivatives resulting from the demethylation of donepezil and three hybrids combining lipoic acid (LA) with donepezil. Phenolic or catecholic functions are known for their ability to scavenge radicals, while LA hybrids exhibit a broad-spectrum antioxidant capacity attributed to the presence of 1,2-dithiolane [26]. All new compounds have been evaluated for their AChE activity, their antioxidant effect, and their neuroprotective effect. More precisely, inhibition of AChE activity has been evaluated on hAChE by the Ellman assay and the binding mode of the most effective compounds has been approached by molecular modelling. The DPPH and ABTS assays have been employed to assess the radical-scavenging potential and in addition, the ORAC assay was used to evaluate the capacity to quench peroxyl radicals and prevent oxidation. The neuroprotective effect was evaluated on the human neuroblastoma cells SK-N-BE(2) by the DCFFH-DA test after an exposure to tert-butylhydroperoxide (t-BHP).

Results and Discussion

Synthetic pathway

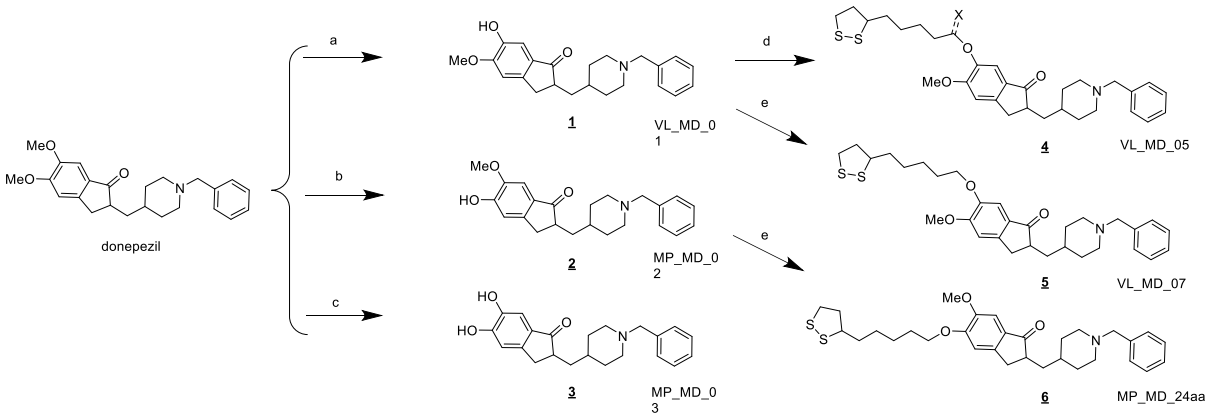

Fig. 1: synthesis of compounds **1** to **6**. Reagents and conditions: a) EtSNa, DMF, 70°C, 5h, 72%; b) HBr aq. 48%, reflux, 12h, 25%; c) BBr_3, - 78°C, DCM, 20h, 54%; d) i)Lipoic acid, oxalyl chloride, DMF cat, DCM, 0°C to room temp., 1h; ii) , Et_3N, DCM, 0°C to room temp., 3h, 64% for two steps; e) ii) Lipoic alcool, mesyl chloride, Et_3N; CH_2Cl_2, 0°C to room temperature, 64%, ii) K_2CO_3, DMF, room temp. **5**: 61%, **6**: 41%.

Selective demethylation of donepezil at position 6, leading to the 6-O-desmethyldonepezil **1**, is obtained in high yield with sodium ethanethiolate in DMF at 70°C [27]. Selective demethylation of methoxy at position 5, leading to 5-O-desmethyldonepezil **2**, is obtained under reflux in a concentrated solution of hydrobromic acid with moderate yield [28]. Boron tribromide, even at low temperature, provides a complete demethylation leading to the catechol derivative **3**. The 6-O-desmethyl donepezil **1** is then esterified in DCM in the presence of DMAP and Et_3N in a mixture of DCM and DMF by lipoic acid converted into lipoyl chloride by oxalyl chloride and a catalytic amount of DMF in DMC. Lipoic alcohol, obtained by catechol borane reduction of lipoic acid as described by Kabalka *et al*. [29], was mesylated and engaged in substitution with 6-O-desmethyldonepezil **1** and 5-O-desmethyldonepezil **2** giving respectively compounds **5** and **6**.

AChE inhibition

All compounds were tested for their inhibitory activities toward human AChE (Table 1) using Ellman's method [30]. Demethylated derivatives **1** to **3** show poor inhibition of acetylcholinesterase. The result of 6-O-desmethyl donepezil **1** is quite unexpected as this compound was previously described as an active metabolite on rat homogenate [31] and this information has been widely reported after. LA – donepezil hybrids **4**, **5**, and **6** display high inhibition of acetylcholinesterase, with an IC_{50} of respectively 27.8, 7.63 nM, and 9.12 nM. Compound **4** links the lipoic and donepezil units via a carboxylic ester function, and its activity is slightly weaker than that of compounds **5** and **6**, which link the donepezil and lipoic units via an ether oxide function. These results complement those of Green *et al*. [32] who found a moderate activity of alkyl adducts compared to aromatic adducts of 6-O-desmethyldonepezil on eeAChE. More interestingly, it shows that the hybrids designed using this approach have equivalent activity to donepezil [33].

Table 1: hAChE inhibition of compounds **1** to **6**

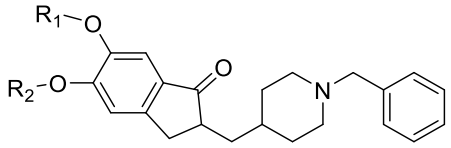

cpd	R_1	R_2	IC_{50} ± SD (nM)
1	H	Me	871.6 ± 77.8
2	Me	H	773.5 ± 29.0
3	H	H	1805.0 ± 170.1

4	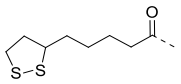	Me	27.8 ± 2.81
5	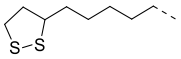	Me	7.63 ± 1.35
6	Me	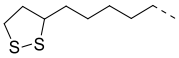	9.12 ± 1.43
DPZ	Me	Me	9.89 ± 1.06

We performed docking simulations and quantum chemistry calculations to predict the binding mode of the most promising compounds (**4**, **5** and **6**) and our reference (donepezil DPZ) in the pocket of the enzyme. The docking calculations, further confirmed by DFT structure optimisations, show that compounds **4**, **5** and **6** can bind to the pocket as tightly as donepezil. The complexation energy differences with respect to that of donepezil are indeed very limited: -0.3, +0.8 and +1.1 kcal mol^{-1}, respectively. These values contribute to explain that these three compounds display a similar activity as donepezil. However, interestingly, the calculations show that compounds **4**, **5** and **6** can bind to hAChE in two very different ways, one similar to that of donepezil, the other one very different.

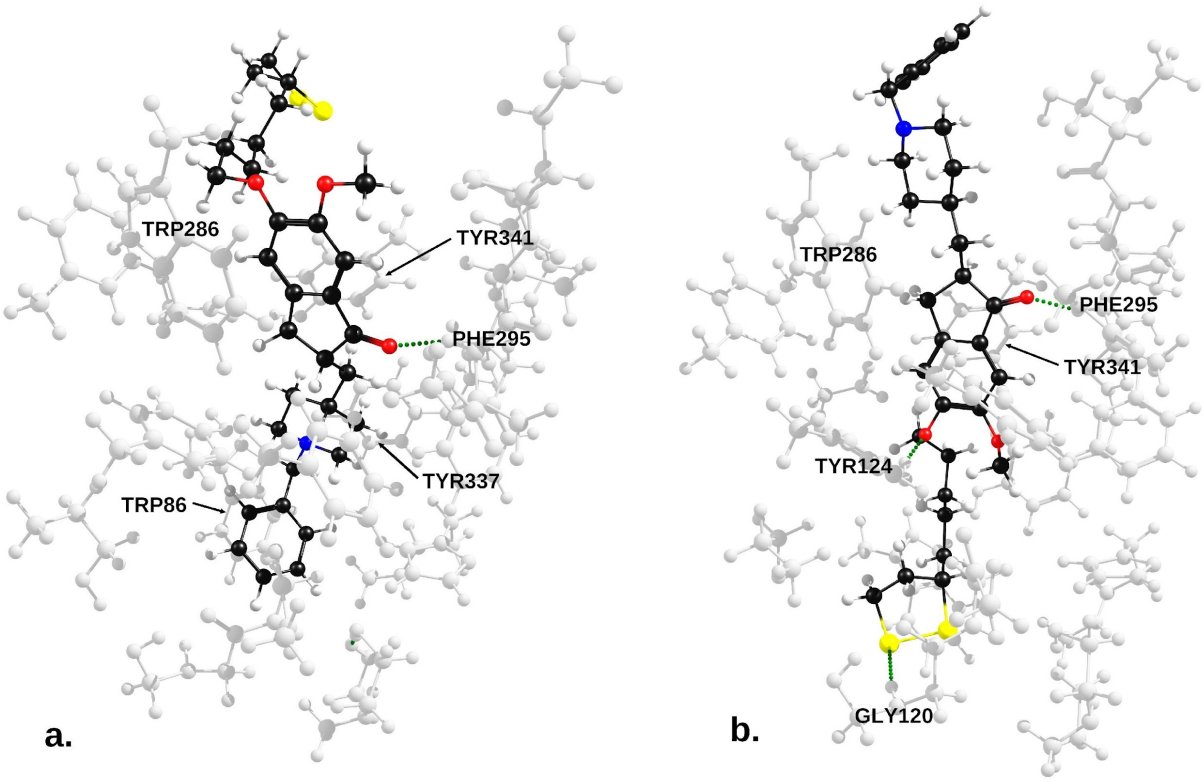

Fig. 2: "regular" (a) and "upside down" (b) conformations of compound **6** inside the hAChE pocket. Hydrogen bonds between the inhibitor and the enzyme are shown in green dotted lines. The atoms of the enzyme are shown in white for clarity reasons. The entrance of the enzyme pocket is located at the top of both illustrations.

In the first binding mode, hereafter named "regular", the indanone macrocycle adopts the same conformation as donepezil in the X-ray diffraction structure [25]. As an example, the case of compound **6** is illustrated in **Fig. 2a**. This position allows a strong aromatic stacking with amino acids TRP286 and TYR341, and a hydrogen bond with the amino group of PHE295. The nitrogen atom of the piperidine ring also interacts with TYR337 in a nitrogen cation / pi bonding type. At the bottom of the pocket, the phenyl end of the inhibitors is also found – in most cases – in the same orientation as with donepezil, pi-stacked with TRP86. Interestingly, the case of the lipoic chain is totally different as it is able to adopt various conformations (**Fig. 3**) of very similar energies (docking scores ranging between -11.1 and -10.9 kcal mol^{-1}). In other words, the chain is free to explore a large part of the space surrounding the entrance of the pocket.

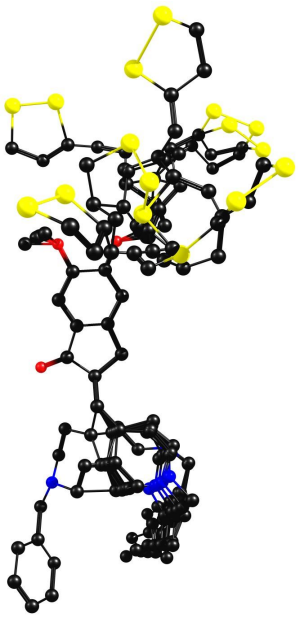

Fig. 3: overlay representation of the best 8 docking poses of compound **6** in the hAChE pocket. Enzyme atoms and hydrogen atoms of the inhibitor were omitted for the sake of clarity.

In the second binding mode, named "upside down" (**Fig. 2b**), the lipoic chain of the inhibitor is buried into the pocket and the phenyl end lies outside the cavity. Despite the reversed orientation of indanone, aromatic stacking with TRP286 and TYR341 and H-bond with PHE295 are preserved. The lost interaction between the phenyl end of the inhibitor and TRP86 is energetically compensated (**Table 2**) for compounds **4** and **5** by the creation of two hydrogen bonds: one donated by the amino group of GLY120 to a sulfur atom of the dithiolane ring, and the other between the alcohol of TYR124 and ether oxide oxygen. For this binding mode,

compound **6** displays a weaker affinity with hAChE than **4** and **5**, because the substitution of position R_2 rather than R_1 (**Table 1**) leads to steric effects with amino acids TRP86, ASP74 and TYR341.

Table 2: Complexation energies (in kcal mol^{-1}) of compounds **4**, **5** and **6** with respect to that of donepezil (DPZ), for the "regular" and "upside down" binding modes

Compound	Relative complexation energy (kcal mol^{-1})	
	regular	upside down
4	+1.7	-0.3
5	+2.3	+0.8
6	+1.1	+5.8
DPZ	0.0	

Antioxidant activity and neuroprotective effect

The ability to capture radicals of each compound was assessed by the DPPH [34,35] and ABTS [36] assays, which measure the extinction efficiency of a stable radical, measured in EC_{50}. The ability to prevent oxidative damage is assessed using the ORAC assay [37,38], which measures the effectiveness in protecting fluorescein from degradation, expressed in equivalent of trolox, a synthetic vitamin E analog. Radical scavenging activity of the 6-O-desmethyldonepezil **1** requires high concentration of 400 µM and 151.9 µM, respectively in DPPH and ABTS assays. However, it is 9 times more potent than trolox in protecting against oxidation in the ORAC assay. The 5-O-desmethydonepezil **2** and catechol derivatives **3** have a capacity to scavenge radicals at lower concentrations, respectively 32.5 µM and 29.5 µM in the DPPH assay and respectively 8.5 µM and 12.3 µM in the ABTS assay, close to the quercetin reference compounds [39]. However, they have a lesser protective effect in ORAC assay, only twice that of trolox [37,38]. As expected, lipoic acid [40] and LA-donepezil derivatives display neither radical scavenging activity on DPPH or ABTS assays nor protective effect on ORAC assay (**Table 3**). Indeed, in situ reduction of thiolane is needed therefore cell culture assay is required.

Table 3: Antioxidant activity of compounds **1** to **6**

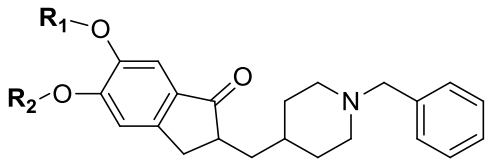

	R1	R2	DPPH (EC50 in µM)	ABTS (EC50 in µM)	ORAC (equiv trolox)
1 MD_01	H	Me	> 400	151.9 ± 5.1	9.4 ± 0.9
2 MD_02	Me	H	32.5 ± 0.9	8.5 ± 0.5	2.1 ± 0.2
3 MD_03	H	H	29.5 ± 0.2	12.3 ±0.3	2.2 ± 0.2
4 MD_05	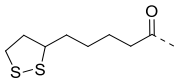	Me	> 400	> 400	< 0.5
5 MD_07	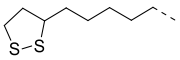	Me	> 400	> 400	< 0.5
6 MD_24aa	Me	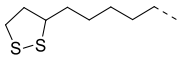	> 400	> 400	< 0.5
DPZ	Me	Me	> 1000	> 1000	< 0.5
quercetin			13.8 ± 0.8	3.4 ± 0.6	4.0 ± 0.1
lipoic acid					
vitamin E			27.5 ± 0.6	15.5 ± 0.7	1

The potential of the tested compounds to protect neuronal cells from oxidative stress was evaluated through their capacity to decrease ROS production induced by *t*-BHP in SK-N-BE(2) cell line. The optimal concentration of *t*-BHP was chosen beforehand in order to lead to a moderate cytotoxicity, with the possibility to be reversed by the addition of the tested compounds. Thus, SK-N-BE(2) cultures was treated for 3h with *t*-BHP at 300 µM and 150 µM. These concentrations corresponded to the lowest concentrations leading to a statistically significant decrease in cell viability, as assessed by MTT assay ($p \leq 0.05$, data not shown). Prior to the protective assay, direct cell toxicity of the selected compounds was evaluated on HepG2 and SK-N-BE(2) up to 100 µM, showing no cytotoxicity of the tested compounds and the reference compounds in both cell lines.

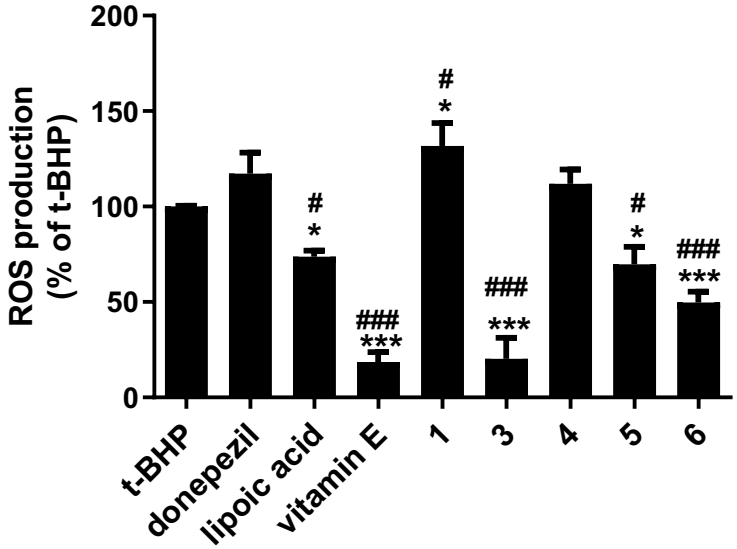

Fig. 4: Effects of the tested compounds and reference compounds on ROS production in SK-N-BE(2) cell cultures co-treated with *t*-BHP for 3h. ROS production was determined by DCFH-DA assay. Data were normalized as a percentage of *t*-BHP-treated cells and are expressed as the means ± SEM from at least three different cultures. T-BHP was used at 300 and 150 µM in SK-N-BE(2) cells. All compounds were assayed at 100 µM. *p<0.05, **p<0.01, and ***p<0.001 compared with control (*t*-BHP-treated cells). #p<0.05, ##p<0.01, and ###p<0.001 compared with donepezil-treated cells.

The ability of the tested compounds to reverse the ROS production induced by *t*-BHP was evaluated using the DCFH-DA test on SK-N-BE(2) cells (**Fig. 4**). A significant increase of ROS production was obtained with *t*-BHP (2.1 +/- 0.2 fold increases for SK-N-BE(2) cells as compared to the control cells). The co-treatment of cells with *t*-BHP and the reference compounds lipoic acid and vitamin E, both used as antioxidant molecules, led to a marked decrease of ROS production in both cells. As expected, donepezil has no effect on *t*-BHP-induced ROS production [41]. Unexpectedly, compound **1** significantly increased the production of ROS while the catechol derivative **3** led to ROS levels comparable to those obtained with the well-known antioxidant vitamin E. Surprisingly, compound **4**, the carboxylic ester derivative of LA, had no significant effect, suggesting that LA is not released by hydrolysis under cell culture conditions. Fortunately, compounds **5** and **6**, lipoic ether oxides, significantly reduced ROS production, leading to a more pronounced effect than with lipoic acid in both cell lines. It suggests that 6-O-desmethyldonepezil could be an efficient platform for development of donepezil hybrid.

Conclusions

Six compounds, including three demethylated derivatives of donepezil and three innovative LA-donepezil hybrids, were synthesized and evaluated for AChE inhibition and their antioxidant and neuroprotective capacity. Although they retain the ability to bind PAS by pi-stacking, the hydrophilic character considerably reduces the affinity for PAS, which is highly lipophilic, in favor of the aqueous solvent. In this line, LA - donepezil hybrids regain a lipophilic character and display high affinity for AChE. In this series, the capacity for radical scavenging is predictive of an antioxidant effect, but does not fully correlate with the neuroprotective effect, which must at least be verified. Surprisingly, 6-O-desmethyldonepezil, the main metabolite of donepezil, even appears to have a deleterious effect on protection against ROS production. Therefore, the metabolites of donepezil cannot have their own neuroprotective effect. In contrast, LA-donepezil hybrids combine both AChE inhibition and a neuroprotective effect at least as strong as LA. Thus, the alkylation of desmethyldonepezil can serve as a molecular framework for the development of MTDL in the context of Alzheimer disease without the need for extensive pharmacomodulation.

Experimental section

Synthesis

Starting materials, reagents and analytical grade solvents were purchased from Sigma-Aldrich and Acros organics. Reactions were monitored by TLC using Merck Kieselgel 60 F_{254} aluminium plates. IR spectra were performed on a Perkin Elmer Spectrum65 with UATR and principal absorptions are given in cm^{-1}. ^{1}H and ^{13}C NMR spectra were recorded in the specified deuterated solvent respectively at 400 MHz and 100 MHz on a Brucker Ascend 400. Chemical shifts are expressed in parts per million (δ) relative to the solvent signal and the coupling constants *J* are given in Hertz (Hz). The following abbreviations were used: s (singlet), d (doublet), t (triplet), q (quadruplet), dd (doublet of doublet), m (multiplet), bs (broad signal). ESI – MS analyses were carried out at the Service Commun d'Analyse, ICMR – UMR CNRS 6229 – 51 100 Reims.

2-[(1-benzylpiperidin-4-yl)methyl]-2,3-dihydro-6-hydroxy-5-methoxyinden-1-one ***(1)***

VL_MD_01

To a mixture of 380 mg of 2-[(1-benzylpiperidin-4-yl)methyl]-5,6-dimethoxy-2,3-dihydroinden-1-one **(2)** (1 mmol, 1eq.) in 15 mL of dry DMF are added 420 mg of sodium ethanthiolate (5 mmol, 5 eq.) and the reaction is stirred for 5 hours at 70 °C. The crude product is concentrated under vacuum and then diluted in water and extracted with dichloromethane. The extract was washed with brine, dried over anhydrous Na_2SO_4 and evaporated under vacuum. The obtained solid was recrystallized in ethanol to give title compound (265 mg, 72%) as a white solid. ^{1}H NMR ($CDCl_3$) δ ppm : 7.31 (s, 5H, Bn), 7.15 (s, 1H, I_7), 6.85 (s, 1H, I_4), 6.21 (s_b, 1H, OH), 3.86 (s, 3H, O$\underline{CH_3}$), 3.56 (s, 2H, $C\underline{H_2}Ph$), 3.24-3.10 (m, 1H, I_2), 3.02-2.90 (m, 2H, 2'ax), 2.72-2.56 (m, 2H, I_3), 2.04 (t, J = 10.3 Hz, 2H, 2'eq), 1.93 – 1.86 (m, 1H, 4'), 1.71 (t, J = 14.3 Hz, 2H, 3'ax), 1.54 – 1.22 (m, 4H, 3'eq, 5'). ^{13}C NMR ($CDCl_3$) δ ppm : 207.9, 152.6, 149.2, 147.0, 129.3, 129.0, 128.1, 127.0, 111.0, 104.2, 63.4, 56.2, 53.7, 45.4, 38.6, 34.4, 33.1, 32.9, 31.6. HRMS : *m/z* 366.2065 (Calc. Mass 366.2069). In accordance with [27].

2-[(1-benzylpiperidin-4-yl)methyl]-2,3-dihydro-5-hydroxy-6-methoxyinden-1-one ***(2)***

VL_MD_02

A solution of donepezil base (566 mg, 1.49 mmol) in HBr 48% (8 mL) and AcOH (2 mL) under nitrogen was refluxed. After completion (12h – TLC monitoring), reaction mixture was poured into freezing water and alkalinized with K_2CO_3 to pH = 8 and saturated with NaCl. The product was extracted with ethyl acetate and the extract was washed with brine, dried over anhydrous Na_2SO_4 and evaporated under vacuum. The obtained solid was purified by flash chromatography (CH_2Cl_2 – MeOH 5%) to give a withe solid (134 mg, 25 %). Mp = 160 °C; ^{1}H NMR ($CDCl_3$) δ ppm : 7.35-7.23 (s, 5H, Bn), 7.16 (s, 1H, I_7), 6.89 (s, 1H, I_4), 5.76 (s_b, 1H, OH), 3.90 (s, 3H, O$\underline{CH_3}$), 3.61 (s, 2H, $C\underline{H_2}Ph$), 3.19 (dd, J = 22.8/10.8 Hz, 1H, I_2), 3.05-2.96 (m, 2H, 2'ax), 2.72-2.59 (m, 2H, I_3), 2.15-2.00 (m, 2H, 2'eq), 1.95 – 1.83 (m, 1H, 4'), 1.79-1.65 (m, 2H, 3'ax), 1.59 – 1.19 (m, 4H, 3'eq, 5'). ^{13}C NMR ($CDCl_3$) δ ppm : 207.9 (I1), 153.0 (I5), 149.4 (I7a), 147.3 (I5a), 137.2 (CBn quat), 129.8 (CH x2 Bn), 129.2 (I4a), 128.5 (CH x2 Bn), 127.6 (CH Bn), 111.3 (I7), 104.5 (I4), 63.1 (CH3O), 56.4 (CH2Ph), 53.6 (C2'), 45.5 (I2), 38.8 (I3), 34.3 (C4'), 33.4 (C3'), 32.6 (C5'). HRMS : *m/z* 366.2064 (Calc. Mass 366.2069). In accordance with [28].

*2-[(1-benzylpiperidin-4-yl)methyl]-2,3-hydro-5,6-dihydroxyinden-1-one (**3**)* **VL_MD_03**

To a mixture of 2-[(1-benzylpiperidin-4-yl)methyl]-5,6-dimethoxy-1-indanone **(2)** (379 mg, 1 mmol, 1eq.) in 30 mL of anhydrous dichloromethane was added dropwise 6mL of an anhydrous 1M solution of BBr_3 in THF (6 eq.) at -78 °C under nitrogen atmosphere. The mixture was allowed slowly to warm up to room temperature and stirred overnight. The reaction was quenched by careful addition of brine and product was extracted by ethyl acetate. Organic layers were evaporated under reduced pressure and the product was obtained by flash chromatography (dichloromethane – methanol 5%) as a white solid (189 mg ,54%). ^{1}H NMR ($CDCl_3$) δ ppm : 7.48 – 7.26 (m, 5H, Bn); 6.87 (s, H, I4); 6.69 (s, 1H, I7); 4.19 (s, 2H, CH_2Ph), 3.21 – 3.00 (m, 1H, I2); 3.20 – 3.00 (m, 2H, 2'ax); 3.00 – 2.82 (m, 2H, I2); 2.00 – 1.55 (m, 5H, 3', 4'); 1.45 – 1.06 (m, 4H, 5', 3'eq). HRMS : *m/z* 352.1897 (Calc. Mass 352.1913).

*2-((1-benzylpiperidin-4-yl)methyl)-6-methoxy-3-oxo-2,3-dihydro-1H-inden-5-yl 5-(1,2-dithiolan-3-yl)pentanoate (**4**) VL_MD_05*

To a solution of lipoic acid (125 mg, 0.61 mmol, 1 equiv.) at 0°C in dry dichloromethane, was added oxalyl chloride (62 µL, 0.73 mmol, 1.2 equiv.) and dry N,N-dimethylformamide (12 µL, 0.2 eq.). After 30 min, the reaction mixture was allowed to warm up at r.t. After completion of this step (TLC monitoring) the solvent was evaporated. The residue was diluted with dichloromethane and added to a solution of **VL_MD_01** (222 mg, 0.61 mmol, 1 equiv.) and triethylamine (342 µL, 2.44 mmol, 4 equiv.) at 0°C in dry dichloromethane. After 3h at r.t., reaction mixture was washed with $NaHCO_3$ 5% and brine. The organic layer was dried over sodium sulfate, filtered and concentrated in vacuo. Pure product was obtained by flash chromatography (CH_2Cl_2) as a white solid (216 mg, 64%). ^{1}H NMR ($CDCl_3$) δ ppm : 7.51 – 7.42 (m, 2H, Bn); 7.38 – 7.31 (m, 3H, Bn); 7.20 (s, 1H, I4); 7.06 (s, 1H, I7); 3.88 (s, 2H, CH2Ph); 3.81 (s, 3H, CH3O); 3.56 (quint, J = 9.2 Hz, 1H, CHRS); 3.22 – 3.02 (m, 5H, I2, CH2S, CH2CO); 2.72 – 2.53 (m, 4H, I3, 2'ax); 2.51 – 2.33 (m, 3H, lip); 1.92 – 1.31 (m, 14H, 2'eq, 4', 3', 5', lip). ^{13}C NMR ($CDCl_3$) δ ppm : 207.5 (I1), 171.0 (COO), 151.4 (I6), 146.5 (I5), 146.0 (I7a), 134.6 (Bnquat), 131.8 (I4a), 130.6 (Bn), 128.0 (Bn), 128.8 (Bn), 120.5 (I7), 105.8 (I4), 61.5 (CH2Ph), 56.3 (CH3O), 56.1 (lip6=CHRS), 52.5 (2'), 45.0 (I2), 40.2 (CH2S), 38.5 (I3), 37.8 (lip), 34.6 (lip), 33.8 (lip), 33.1 (5'), 32.7 (4'), 29.2 (3'), 28.6 (lip), 24.6 (lip). HRMS : *m/z* 554.2402 (Calc. Mass 554.2399)

5-(1,2-dithiolan-3-yl)pentyl methanesulfonate MP_MD-13a

To a solution of lipool (prepared as [22]) in dry DCM at 0°C and under nitrogen atmosphere, Et_3N (110 µL, 0.79 mmol, 1.2 equiv.) and mesyl chloride (61 µL, 0.79 mmol, 1.2 equiv.) were added. The mixture was allowed slowly to warm up to room temperature and stirred until completion of the reaction (1.5h, TLC monitoring). The reaction mixture was washed with a solution of K_2CO_3 10% and brine, dried over anhydrous Na_2SO_4 and evaporated under vacuum. The product was purified by flash chromatography (dichloromethane) as a translucent oil (115 mg ,64 %). ^{1}H NMR ($CDCl_3$) δ ppm : 4.21 (t, J = 8.4 Hz, 2H, lip1); 3.55 (quint, J = 9.0 Hz, 1H, CHRS); 3.25 – 3.05 (m, 2H, lip2); 2.99 (s, 3H, CH_3SO_2); 2.45 (sex, J = 9.0 Hz, 1H, lip); 2.05 – 1.30 (m, 9H).

6-O-desmethyldonepezil alkylation

VL_MD_01 or **VL_MD_02** (258 mg, 0.71 mmol, 1 equiv.) was suspended in dry DMF and DCM was added until dissolved. Potassium carbonate (293 mg, 2.12 mmol, 3 equiv.) finely pulverized was added and the reaction mixture was stirred for 15 min. Then **MP_MD-13a** (210 mg, 0.78 mmol, 1.1 equiv.) was suspended in dry DMF, DCM was added until dissolved and the solution was added to the reaction mixture. The reaction mixture was stirred until completion (TLC monitoring), then diluted with water, and extracted with DCM. Organic layer was washed three times with water and once with brine, dried over sodium sulfate, filtered, and solvent was removed under reduced pressure. The product was purified by flash chromatography (DCM – MeOH 4%) to give the desired product as a white solid (258 mg, 61% for **MP_MD_20aa** and 186 mg, 41 % for **MP_MD_24aa**).

6-((5-(1,2-dithiolan-3-yl)pentyl)oxy)-2-((1-benzylpiperidin-4-yl)methyl)-5-methoxy-2,3-dihydro-1H-inden-1-one (**5**)

MP_MD_20aa: ^{1}H NMR ($CDCl_3$) δ ppm : 7.32 – 7.19 (m, 5H, Bn); 7.13 (s, 1H, I4); 6.80 (s, 1H, I7); 4.06 (t, J= 6.4 Hz, 2H, CH2O); 3.85 (s, 3H, CH3O); 3.56 (quint, J = 6.4 Hz, 1H, CHRS); 3.49 (s, 2H, Bn); 3.23 – 3.05 (m, 3H, I2, CH2S); 2.92 – 2.83 (m, 2H, 2'ax); 2.70 – 2.62 (m, 2H, I2); 2.44 (sex, 1H, lip); 2.04 – 1.80 (m, 6H, 2'eq, 4', lip); 1.78 – 1.59 (m, 4H, 3'ax, lip); 1.58 – 1.40 (m, 5H, 3'eq, lip); 1.39 – 1.20 (m, 3H, 5', 3'eq). ^{13}C NMR ($CDCl_3$) δ ppm : 208.0 (I1), 155.2 (I6), 149.8 (I5), 148.9 (I7a), 138.6 (Bnquat), 129.4 (Bn), 129.3 (I4a), 128.3 (Bn), 127.1 (Bn), 108.5 (I7), 104.8 (I4), 69.1 (CH2O), 63.6 (CH2Ph), 56.7 (CH3O), 56.3 (lip6=CHRS), 54.0 (2'), 45.7 (I2), 40.5 (CH2S), 38.9 (I3), 38.7 (lip7), 35.0 (lip5), 34.7 (4'), 33.5 (lip4), 33.2 (5'), 29.2 (3'), 28.9 (lip2), 26.0 (lip3). HRMS : *m/z* 540.2593 (Calc. Mass 540.2606).

5-((5-(1,2-dithiolan-3-yl)pentyl)oxy)-2-((1-benzylpiperidin-4-yl)methyl)-6-methoxy-2,3-dihydro-1H-inden-1-one (**6**)

MP_MD_24aa: ^{1}H NMR ($CDCl_3$) δ ppm : 7.34 – 7.25 (m, 5H, Bn); 7.12 (s, 1H, I4); 6.82 (s, 1H, I7); 4.00 (t, J= 9.2 Hz, 2H, CH2O); 3.91 (s, 3H, CH3O); 3.61-3.51 (m, 1H, CHRS); 3.49 (s, 2H, Bn); 3.26 – 3.04 (m, 3H, I2, CH2S); 2.94 – 2.83 (m, 2H, 2'ax); 2.71 – 2.61 (m, 2H, I2); 2.49-2.37 (m, 1H, lip); 1.99 – 1.73 (m, 6H, 2'eq, 4', lip); 1.72 – 1.61 (m, 4H, 3'ax, lip); 1.55 – 1.42 (m, 5H, 3'eq, lip); 1.36 – 1.21 (m, 3H, 5', 3'eq). ^{13}C NMR ($CDCl_3$) δ ppm : 208.0 (I1), 156.0 (I6), 149.0 (I7a), 148.8 (I5), 133.2 (Bnquat), 129.5 (Bn), 128.4 (Bn), 127.5 (I4a), 127.2 (Bn), 107.7 (I7), 105.7 (I4), 69.0 (CH2O), 63.6 (CH2Ph), 56.7 (CH3O), 56.4 (lip6=CHRS), 53.9 (2'), 45.6 (I2), 40.4 (CH2S), 38.9 (I3), 38.7 (lip7), 35.0 (lip5), 34.6 (4'), 33.5 (lip4), 33.1 (5'), 29.2 (3'), 28.9 (lip2), 26.0 (lip3). HRMS : *m/z* 554.2402 (Calc. Mass 554.2399)

Inhibition of hAChE

The method of Ellman *et al*. was followed [23]. Human erythrocyte AChE was obtained from Sigma–Aldrich. Stock solutions were prepared by dissolving lyophilized enzymes in phosphate buffer solution (pH = 8.0). Solutions of tested compounds were prepared starting from 10 mM stock solutions in DMSO diluted with aqueous assay medium to a final content of organic solvent always under 1%. Five concentrations of each compound were used in order to obtain an inhibition of hAChE comprised between 20% and 80%.

The assay solution in a total volume of 3 mL consisted of 0.1 M phosphate buffer solution pH = 8.0 and contained 5,5'-dithio-bis(2-nitrobenzoic acid), DTNB (2 625 µL, 0.35 mM final concentration), sample (3 µL, 0.01 to 10 µM final concentration), hAChE (29 µL, 0.035 u.i./mL final concentration) and substrate (acetylthiocholine iodide, 105 µL, 0.35 mM final concentration). Increasing concentration of tested compounds were added to the assay solution and pre-incubated for 10 min at room temperature with the enzyme followed by the addition of substrate and absorbance was measured after 15 min. Assays were done with a blank containing all components except the enzyme in order to account for non-enzymatic reactions and one sample where only inhibitor was replaced by the buffer solution was always present to yield the 100% of hAChE activity (control). Absorbance values were recorded at 412 nm in quadruplicate and the values were averaged. The percentage of inhibition was calculated as $[(A_{control} - A_{blank}) - (A_{sample} - A_{blank})/ (A_{control} - A_{blank})]$ x100.

Bovine Serum Albumin (BSA) is usually added up to 0.5% of the total reaction volume to reduce the coating of the target enzyme during the incubation. In our assay, no obvious effect from BSA on the activity of the compounds was found. This indicates that the new compounds selectively inhibit the target enzymes but do not interact with BSA.

The concentration of compound which determined 50% inhibition of the AChE activity (IC_{50}) was calculated using a sigmoidal hill slope model.

Computational chemistry methods

Docking

As a first approach, we performed docking simulations with the Autodock Vina software [32], using the X-ray diffraction structure 4EY7 of hAChE by Cheung & al. [18]. The ligands and the protein structure were prepared for docking using MGLTools-1.5.6.

Quantum chemistry modelling

The subtle interaction of donepezil – and its derivatives – with the active site of AChE lead us to choose advanced quantum chemistry methods, in order to obtain accurate complexation energies. We used the same hAChE structure [25] as for our docking calculations to build a 281-atoms model representing all or part of 24 amino acids that form the inner layer of the enzyme pocket (TYR72, ASP74, TRP86, GLY120, GLY121, GLY122, PHE123, TYR124, SER125, GLU202, SER203, TRP286, GLU292, SER293, VAL294, PHE295, ARG296, PHE297, TYR337, PHE338, LEU339, TYR341, HIS447 and GLY448). Input structures that include inhibitors mostly came from docking poses, but some were built manually to ensure a comprehensive exploration of the phase space. For each inhibitor (DPZ or compounds **4**, **5** or **6**), both enantiomers R and S were considered. In all calculations, we froze the position of 34 of these atoms to take into account the rigidity of the active site, but the side chains of the amino acids could freely rotate and reorient. No constraints were applied to the inhibitor either. Solvation was computed using the IEFPCM solvent model [33–35].

All calculations were carried out with the Gaussian 09 program [42]. The level of theory used for structure optimizations was DFT(B3LYP)/6-31G(d).

Complexation energies were calculated and given with respect to that of the reference, donepezil:

$$Ecomp(i) = E(AChE+i) – E(i) – E(AChE+donepezil) + E(donepezil)$$

Therefore, in our case, a negative complexation energy means that compound *i* displays a better affinity with AChE than donepezil, and vice versa.

DPPH free radical scavenging activity

Assay for the scavenging of stable free radical 1,1-diphenyl-2-picrylhydrazyl (DPPH) was done as previously reported [34,35]. A freshly prepared solution of DPPH (0.15 mM, 2.7 mL) in methanol was added to a methanol solution of tested compounds or quercetin as a reference compound at concentrations in order to obtain an activity comprised between 20% and 80%. The mixture was stirred in the dark at room temperature for 2h and the absorbance was measured in triplicate at 517 nm. RSA%, Radical Scavenging Activity was calculated as $[(A_{control} - A_{sample})/A_{control}]x100$ where $A_{control}$ represents absorbance of control without test sample and A_{sample} represents absorbance in the presence of the test sample. EC_{50} values, calculated from linear fit, is the concentration of compounds required for scavenging 50% of the DPPH radicals in the solution.

2'-azinobis-(3-ethylbenzothiazoline-6-sulfonate), ABTS – Free Radical Scavenging Assay

The ABTS free radical scavenging assay was adapted from Re et al. [36]. A solution of $K_2S_2O_8$ (2.45 mM) and ABTS (7 mM) was prepared and kept at room temperature in the dark for 12-16h. Extemporaneous dilution of the $ABTS^{\bullet+}$ solution was carried out to an absorbance of 0.70 ± 0.02 at 734 nm at room temperature. To a solution of $ABTS^{\bullet+}$ (2.9 mL) was added 100 µL of ethanol for blank, Trolox for control or compound at concentration between 300 and 1 µM (final concentration). The mixture was mixed thoroughly at room temperature and the absorbance was recorded after 6 min at 734 nm on a plate reader (Varioskan Flash Plate Reader – Thermo Scientific).

The scavenging effect was calculated as $1-\frac{A_{CA}-A_C}{A_A}$ where A_{CA} is the absorption of compounds and $ABTS^{\bullet+}$, A_C is the absorbance of the compound without $ABTS^{\bullet+}$ and A_A is the absorption of $ABTS^{\bullet+}$ without the compound. The concentration of compound necessary to

decrease the initial $ABTS^{\bullet+}$ concentration by 50%, named EC_{50}, has been calculated from regression equation.

Oxygen Radical Antioxidant Capacity – Fluorescein (ORAC-FL)

The ORAC-FL method developed by Ou et al. [37] modified by Dávalos et al. [38] was followed using Varioskan plate reader with automatic injectors (Varioskan Flash Plate Reader – Thermo Scientific).

The assay was carried out in 75 mM phosphate buffer at pH 7.4 in 96-well microplate with a final volume of 200 µL. 20 µL of PBS or Trolox solution (1, 2, 4 and 8 µM – final concentration) or compound solution (0.1, 0.2, 0.4, 0.6, 0.8, 1.0 µM – final concentration) were incubated with 120 µL of Fluorescein (70 nM – final concentration) for 15 min at 37°C.

60 µL of AAPH (12mM – final concentration) were rapidly added using embedded injectors and fluorescence was recorded every minute for 80 min (excitation length: 485 nm and emission length: 535 nm) with automatic shaking prior to each reading. Reaction mixtures were prepared in quadruplicate and three independent assays were performed for each compound.

Area under the fluorescence decay curves were determined by Excel software (Microsoft) as follow: $AUC = 1 + \sum_{i=1}^{i=80} f_i / f_0$ where f_i is the fluorescence read at time and f_0 the initial fluorescence read at 0 min. Net AUC were calculated by subtracting the AUC corresponding to the blank. Regression equations of the net AUC against the antioxidant concentration were determined for each compound. ORAC-FL values, expressed as Trolox equivalent, are the ratio of the slopes of the regression lines of the compound and Trolox.

Cells culture assays

Cell lines and reagents

HepG2 and SK-N-BE(2) cells were obtained from the American Type Culture Collection (Manassas, VA, USA). 3-(4,5-dimethylthiazol-2-yl)-2,5-diphenyltetrazolium bromide (MTT) was purchased from Sigma-Aldrich (France). 2',7'-Dichlorofluorescein diacetate (DCFDA) was procured from Molecular Probes (Eugene, OR, USA).

HepG2 and SK-N-BE(2) Cell Culture and Treatment

HepG2 cells were seeded in 96-well culture plates at a density of 6×10^4 cells per well in EMEM medium supplemented with 10% fetal bovine serum (FBS), 1% non-essential amino acids, 100 units/mL penicillin and 10 µg/mL streptomycin (Dutscher, France). After 24 h of incubation, the cultures were treated with 100 µl of the tested compounds or DMSO (0.1%) in the same medium without FBS. SK-N-BE(2) cells were seeded in 96-well culture plates at a density of 12×10^4 cells per well in DMEM/F12 (1:1) medium supplemented with 10% fetal bovine serum, 100 units/mL penicillin and 10 µg/mL streptomycin (Dutscher, France). After 48h of incubation, the cultures were treated with 100 µl of the test compounds or DMSO (0.1%) in the same medium without FBS.

MTT Cell Viability Test

Following 3h of treatment, the percent of cell viability was measured by an MTT assay in HepG2 and SK-N-BE(2) cells. The media were replaced by an MTT solution (100 µL/well at 0.5 mg/mL) and incubated during 2h at 37°C. MTT was removed and 100 µL DMSO was distributed per well. The absorbance was read at 570 nm by microplate spectrophotometry (BioTek). Cell viability was expressed as percentage over controls (DMSO).

Measurement of intracellular ROS levels

The intracellular ROS levels were measured using the cell permeable probe, 2',7'-dichlorofluorescein-diacetate (DCFH-DA), which is easily oxidized to fluorescent dichlorofluorescein (DCF) by intracellular ROS. Briefly, HepG2 and SK-N-BE(2) cells were seeded in 96-well plates as described above. Following 24h (HepG2) or 48h (SK-N-BE(2)) of incubation, DCFH-DA (100 µL/well at 10 µM) was added for 45 min at 37°C in the dark. Cells were washed twice with PBS containing 10 mM glucose and then cells are exposed for 3h to the tested compounds (100 µM) with t-BHP (300 µM for HepG2 or 150 µM for SK-N-BE(2)) in their respective culture media without FBS. The fluorescence was regularly read by a fluorescence spectrophotometer (BioTek) at 485 nm (excitation) and 530 nm (emission).

Statistical analysis

GraphPad Prism version 5.03 (GraphPad software) was used for statistical analysis. Statistical comparison between the different groups was made using one-way ANOVA followed by Dunnett's post-hoc test. $P < 0.05$ was considered statistically significant.

REFERENCES

[1] C. Reitz, C. Brayne, R. Mayeux, Epidemiology of Alzheimer disease, Nat. Rev. Neurol. 7 (2011) 137–152. https://doi.org/10.1038/nrneurol.2011.2.

[2] P.T. Nelson, I. Alafuzoff, E.H. Bigio, C. Bouras, H. Braak, N.J. Cairns, R.J. Castellani, B.J. Crain, P. Davies, K.D. Tredici, C. Duyckaerts, M.P. Frosch, V. Haroutunian, P.R. Hof, C.M. Hulette, B.T. Hyman, T. Iwatsubo, K.A. Jellinger, G.A. Jicha, E. Kövari, W.A. Kukull, J.B. Leverenz, S. Love, I.R. Mackenzie, D.M. Mann, E. Masliah, A.C. McKee, T.J. Montine, J.C. Morris, J.A. Schneider, J.A. Sonnen, D.R. Thal, J.Q. Trojanowski, J.C. Troncoso, T. Wisniewski, R.L. Woltjer, T.G. Beach, Correlation of Alzheimer Disease Neuropathologic Changes With Cognitive Status: A Review of the Literature, J. Neuropathol. Exp. Neurol. 71 (2012) 362–381. https://doi.org/10.1097/NEN.0b013e31825018f7.

[3] A. Kumar, A review on Alzheimer's disease pathophysiology and its management: an update, (n.d.).

[4] M.R. Farlow, M.L. Miller, V. Pejovic, Treatment options in Alzheimer's disease: maximizing benefit, managing expectations, Dement. Geriatr. Cogn. Disord. 25 (2008) 408–422. https://doi.org/10.1159/000122962.

[5] M. de Freitas Silva, K.S.T. Dias, V.S. Gontijo, C.J.C. Ortiz, C. Viegas, Multi-Target Directed Drugs as a Modern Approach for Drug Design Towards Alzheimer's Disease: an update, Curr. Med. Chem. (2018). https://doi.org/10.2174/0929867325666180111101843.

[6] M.J. Oset-Gasque, J. Marco-Contelles, Alzheimer's Disease, the "One-Molecule, One-Target" Paradigm, and the Multitarget Directed Ligand Approach, ACS Chem. Neurosci. 9 (2018) 401–403. https://doi.org/10.1021/acschemneuro.8b00069.

[7] W.-J. Huang, X. Zhang, W.-W. Chen, Role of oxidative stress in Alzheimer's disease, Biomed. Rep. 4 (2016) 519–522. https://doi.org/10.3892/br.2016.630.

[8] X. Wang, W. Wang, L. Li, G. Perry, H. Lee, X. Zhu, Oxidative stress and mitochondrial dysfunction in Alzheimer's disease, Biochim. Biophys. Acta 1842 (2014) 1240–1247. https://doi.org/10.1016/j.bbadis.2013.10.015.

[9] M. Rosini, E. Simoni, M. Bartolini, A. Tarozzi, R. Matera, A. Milelli, P. Hrelia, V. Andrisano, M.L. Bolognesi, C. Melchiorre, Exploiting the lipoic acid structure in the search for novel multitarget ligands against Alzheimer's disease, Eur. J. Med. Chem. 46 (2011) 5435–5442. https://doi.org/10.1016/j.ejmech.2011.09.001.

[10] M.L. Bolognesi, A. Cavalli, C. Bergamini, R. Fato, G. Lenaz, M. Rosini, M. Bartolini, V. Andrisano, C. Melchiorre, Toward a rational design of multitarget-directed antioxidants: merging memoquin and lipoic acid molecular frameworks, J. Med. Chem. 52 (2009) 7883–7886. https://doi.org/10.1021/jm901123n.

[11] W. Chen, Y. Wu, S. Zhong, L. Cheng, Q. Li, H. Tang, Anti-neurotoxicity effects of oxoisoaporphine-lipoic acid hybrids, Chem. Biol. Interact. 223 (2014) 45–50. https://doi.org/10.1016/j.cbi.2014.09.005.

[12] M. Digiacomo, Z. Chen, S. Wang, A. Lapucci, M. Macchia, X. Yang, J. Chu, Y. Han, R. Pi, S. Rapposelli, Synthesis and pharmacological evaluation of multifunctional tacrine derivatives against several disease pathways of AD, Bioorg. Med. Chem. Lett. 25 (2015) 807–810. https://doi.org/10.1016/j.bmcl.2014.12.084.

[13] M. Estrada, C. Pérez, E. Soriano, E. Laurini, M. Romano, S. Pricl, J.A. Morales-García, A. Pérez-Castillo, M.I. Rodríguez-Franco, New neurogenic lipoic-based hybrids as innovative Alzheimer's drugs with σ-1 agonism and β-secretase inhibition, Future Med. Chem. 8 (2016) 1191–1207. https://doi.org/10.4155/fmc-2016-0036.

[14] L. Jalili-Baleh, H. Nadri, H. Forootanfar, A. Samzadeh-Kermani, T.T. Küçükkılınç, B. Ayazgok, M. Rahimifard, M. Baeeri, M. Doostmohammadi, L. Firoozpour, S.N.A. Bukhari, M. Abdollahi, M.R. Ganjali, S. Emami, M. Khoobi, A. Foroumadi, Novel 3-phenylcoumarin-lipoic acid conjugates as multi-functional agents for potential treatment of Alzheimer's disease, Bioorganic Chem. 79 (2018) 223–234. https://doi.org/10.1016/j.bioorg.2018.04.030.

[15] M. Rosini, V. Andrisano, M. Bartolini, M.L. Bolognesi, P. Hrelia, A. Minarini, A. Tarozzi, C. Melchiorre, Rational approach to discover multipotent anti-Alzheimer drugs, J. Med. Chem. 48 (2005) 360–363. https://doi.org/10.1021/jm049112h.
[16] L. Holmquist, G. Stuchbury, K. Berbaum, S. Muscat, S. Young, K. Hager, J. Engel, G. Münch, Lipoic acid as a novel treatment for Alzheimer's disease and related dementias, Pharmacol. Ther. 113 (2007) 154–164. https://doi.org/10.1016/j.pharmthera.2006.07.001.
[17] A. Maczurek, K. Hager, M. Kenklies, M. Sharman, R. Martins, J. Engel, D.A. Carlson, G. Münch, Lipoic acid as an anti-inflammatory and neuroprotective treatment for Alzheimer's disease, Adv. Drug Deliv. Rev. 60 (2008) 1463–1470. https://doi.org/10.1016/j.addr.2008.04.015.
[18] K. Ono, M. Hirohata, M. Yamada, Alpha-lipoic acid exhibits anti-amyloidogenicity for beta-amyloid fibrils in vitro, Biochem. Biophys. Res. Commun. 341 (2006) 1046–1052. https://doi.org/10.1016/j.bbrc.2006.01.063.
[19] K. Hager, M. Kenklies, J. McAfoose, J. Engel, G. Münch, Alpha-lipoic acid as a new treatment option for Alzheimer's disease--a 48 months follow-up analysis, J. Neural Transm. Suppl. (2007) 189–193.
[20] B. Sameem, M. Saeedi, M. Mahdavi, A. Shafiee, A review on tacrine-based scaffolds as multi-target drugs (MTDLs) for Alzheimer's disease, Eur. J. Med. Chem. 128 (2017) 332–345. https://doi.org/10.1016/j.ejmech.2016.10.060.
[21] M. Unzeta, G. Esteban, I. Bolea, W.A. Fogel, R.R. Ramsay, M.B.H. Youdim, K.F. Tipton, J. Marco-Contelles, Multi-Target Directed Donepezil-Like Ligands for Alzheimer's Disease, Front. Neurosci. 10 (2016) 205. https://doi.org/10.3389/fnins.2016.00205.
[22] L. Ismaili, B. Refouvelet, M. Benchekroun, S. Brogi, M. Brindisi, S. Gemma, G. Campiani, S. Filipic, D. Agbaba, G. Esteban, M. Unzeta, K. Nikolic, S. Butini, J. Marco-Contelles, Multitarget compounds bearing tacrine- and donepezil-like structural and functional motifs for the potential treatment of Alzheimer's disease, Prog. Neurobiol. 151 (2017) 4–34. https://doi.org/10.1016/j.pneurobio.2015.12.003.
[23] E. Mezeiova, K. Spilovska, E. Nepovimova, L. Gorecki, O. Soukup, R. Dolezal, D. Malinak, J. Janockova, D. Jun, K. Kuca, J. Korabecny, Profiling donepezil template into multipotent hybrids with antioxidant properties, J. Enzyme Inhib. Med. Chem. 33 (2018) 583–606. https://doi.org/10.1080/14756366.2018.1443326.
[24] O. Prezzavento, E. Arena, C. Parenti, L. Pasquinucci, G. Aricò, G.M. Scoto, S. Grancara, A. Toninello, S. Ronsisvalle, Design and Synthesis of New Bifunctional Sigma-1 Selective Ligands with Antioxidant Activity, J. Med. Chem. 56 (2013) 2447–2455. https://doi.org/10.1021/jm3017893.
[25] J. Cheung, M.J. Rudolph, F. Burshteyn, M.S. Cassidy, E.N. Gary, J. Love, M.C. Franklin, J.J. Height, Structures of human acetylcholinesterase in complex with pharmacologically important ligands, J. Med. Chem. 55 (2012) 10282–10286. https://doi.org/10.1021/jm300871x.
[26] E.S. Billgren, R.M. Cicchillo, N.M. Nesbitt, S.J. Booker, 7.07 - Lipoic Acid Biosynthesis and Enzymology, in: H.-W. (Ben) Liu, L. Mander (Eds.), Compr. Nat. Prod. II, Elsevier, Oxford, 2010: pp. 181–212. https://doi.org/10.1016/B978-008045382-8.00137-4.
[27] L. Bhat, P.P. Mohapatra, L. Bhat, Compositions, synthesis, and methods of using indanone based cholinesterase inhibitors, US2008153878 (A1), 2008. https://worldwide.espacenet.com/publicationDetails/biblio?FT=D&date=20080626&DB=EPODOC&locale=en_EP&CC=US&NR=2008153878A1&KC=A1&ND=4 (accessed August 27, 2018).
[28] T. Mezei, G. Simig, G. Lukacs, M. Porcs-Makkay, B. Volk, E. Molnar, F. Hofmanne, Donepezil Salts Suitable for the Preparation of Pharmaceutical Compositions, WO2006030249 (A1), 2006. https://worldwide.espacenet.com/publicationDetails/biblio?FT=D&date=20060323&DB=&locale=&CC=WO&NR=2006030249A1&KC=A1&ND=1 (accessed August 27, 2018).
[29] G.W. Kabalka, J.D. Baker, G.W. Neal, Catecholborane (1,3,2-benzodioxaborole). A versatile reducing agent, J. Org. Chem. 42 (1977) 512–517. https://doi.org/10.1021/jo00423a025.
[30] G.L. Ellman, K.D. Courtney, V. Andres, R.M. Feather-Stone, A new and rapid colorimetric determination of acetylcholinesterase activity, Biochem. Pharmacol. 7 (1961) 88–95.
[31] H. Sugimoto, Y. Tsuchiya, K. Higurashi, N. Karibe, Y. Iimura, A. Sasaki, Y. Yamanishi, H. Ogura, S. Araki, T. Kosasa, A. Kubota, M. Kosasa, K. Yamatsu, Cyclic amine compounds with activity against acetylcholinesterase, US4895841A, 1990. https://patents.google.com/patent/US4895841A/en?oq=US4895841A (accessed July 7, 2021).

[32] K.D. Green, M.Y. Fosso, S. Garneau-Tsodikova, Multifunctional Donepezil Analogues as Cholinesterase and BACE1 Inhibitors, Molecules 23 (2018) 3252. https://doi.org/10.3390/molecules23123252.
[33] R. Azzouz, L. Peauger, V. Gembus, M.-L. Ţînţaş, J. Sopková-de Oliveira Santos, C. Papamicaël, V. Levacher, Novel donepezil-like *N*-benzylpyridinium salt derivatives as AChE inhibitors and their corresponding dihydropyridine "bio-oxidizable" prodrugs: Synthesis, biological evaluation and structure-activity relationship, Eur. J. Med. Chem. 145 (2018) 165–190. https://doi.org/10.1016/j.ejmech.2017.12.084.
[34] P.C. Eklund, O.K. Långvik, J.P. Wärnå, T.O. Salmi, S.M. Willför, R.E. Sjöholm, Chemical studies on antioxidant mechanisms and free radical scavenging properties of lignans, Org. Biomol. Chem. 3 (2005) 3336–3347. https://doi.org/10.1039/B506739A.
[35] M.C. Foti, C. Daquino, C. Geraci, Electron-transfer reaction of cinnamic acids and their methyl esters with the DPPH(*) radical in alcoholic solutions, J. Org. Chem. 69 (2004) 2309–2314. https://doi.org/10.1021/jo035758q.
[36] R. Re, N. Pellegrini, A. Proteggente, A. Pannala, M. Yang, C. Rice-Evans, Antioxidant activity applying an improved ABTS radical cation decolorization assay, Free Radic. Biol. Med. 26 (1999) 1231–1237. https://doi.org/10.1016/S0891-5849(98)00315-3.
[37] B. Ou, M. Hampsch-Woodill, R.L. Prior, Development and Validation of an Improved Oxygen Radical Absorbance Capacity Assay Using Fluorescein as the Fluorescent Probe, J. Agric. Food Chem. 49 (2001) 4619–4626. https://doi.org/10.1021/jf010586o.
[38] A. Dávalos, C. Gómez-Cordovés, B. Bartolomé, Extending Applicability of the Oxygen Radical Absorbance Capacity (ORAC−Fluorescein) Assay, J. Agric. Food Chem. 52 (2004) 48–54. https://doi.org/10.1021/jf0305231.
[39] C. Tian, X. Liu, Y. Chang, R. Wang, T. Lv, C. Cui, M. Liu, Investigation of the anti-inflammatory and antioxidant activities of luteolin, kaempferol, apigenin and quercetin, South Afr. J. Bot. 137 (2021) 257–264. https://doi.org/10.1016/j.sajb.2020.10.022.
[40] F. Zhao, Z.-Q. Liu, Comparison of antioxidant effectiveness of lipoic acid and dihydrolipoic acid, J. Biochem. Mol. Toxicol. 25 (2011) 216–223. https://doi.org/10.1002/jbt.20378.
[41] A. Ahmet, K.A. Hakan, K. Derya, C. Mustafa, O.K. Cansu, D. Adem, Protective Effects of Quercetin in Combination with Donepezil against H2O2-Induced Oxidative Stress in Glioblastoma Cells, Pharm. Chem. J. 56 (2023) 1577–1586. https://doi.org/10.1007/s11094-023-02830-3.
[42] Citation | Gaussian.com, (n.d.). https://gaussian.com/citation/ (accessed January 12, 2024).